https://doi.org/10.5194/egusphere-2022-947
Preprint. Discussion started: 10 October 2022

Responses of elemental content and macromolecule of the coccolithophore *Emiliania huxleyi* to reduced phosphorus availability and ocean acidification depend on light intensity

Yong Zhang[1,*], Yong Zhang[1,§], Shuai Ma[1], Hanbing Chen[2], Jiabing Li[1], Zhengke Li[3], Kui Xu[4], Ruiping Huang[5], Hong Zhang[1], Yonghe Han[1], Jun Sun[6]

[1]College of Environmental and Resource Sciences, College of Carbon Neutral Modern Industry, Fujian Key Laboratory of Pollution Control and Resource Recycling, Fujian Normal University, Fuzhou, China

[2]College of Life Science, Fujian Normal University, Fuzhou, China

[3]School of Food and Biological Engineering, Shanxi University of Science and Technology, Xi'an, China

[4]Hubei Key Laboratory of Edible Wild Plants Conservation and Utilization, Hubei Engineering Research Center of Special Wild Vegetables Breeding and Comprehensive Utilization Technology, College of Life Sciences, Hubei Normal University, Huangshi, China

[5]State Key Laboratory of Marine Environmental Science, College of Ocean and Earth Sciences, Xiamen University, Xiamen, China

[6]Institute for Advanced Marine Research, China University of Geosciences, Guangzhou, China

https://doi.org/10.5194/egusphere-2022-947
Preprint. Discussion started: 10 October 2022

Running head: Physiology and biochemistry of *E. huxleyi*

*Correspondence: Yong Zhang (yongzhang@fjnu.edu.cn)

Keywords: Carbohydrate; CO_2; coccolithophore; elemental content; light intensity; phosphorus availability; protein.

§Email: qsx20211022@student.fjnu.edu.cn

https://doi.org/10.5194/egusphere-2022-947
Preprint. Discussion started: 10 October 2022

Abstract

Global climate change leads to simultaneous changes in multiple environmental drivers in the marine realm. Although physiological characterization of coccolithophores have been studied under climate change, there is limited knowledge on the biochemical responses of this biogeochemically important phytoplankton group to changing multiple environmental drivers. Here we investigate the interactive effects of reduced phosphorus availability (4 to 0.4 μmol L^{-1}), elevated pCO_2 concentrations (426 to 946 μatm) and increasing light intensity (40 to 300 μmol photons m^{-2} s^{-1}) on elemental content and macromolecules of the cosmopolitan coccolithophore *Emiliania huxleyi*. Reduced phosphorus availability reduces particulate organic nitrogen and protein contents under low light intensity, but not under high light intensity. Reduced phosphorus availability and ocean acidification act synergistically to increase particulate organic carbon (POC) and carbohydrate contents under high light intensity but not under low light intensity. Reduced phosphorus availability, ocean acidification and increasing light intensity act synergistically to increase the allocation of POC to carbohydrates. Under future ocean acidification and increasing light intensity, enhanced carbon fixation could increase carbon storage in the phosphorus-limited regions of the oceans where *E. huxleyi* dominates the phytoplankton assemblages. In each light intensity, elemental carbon to phosphorus (C : P) and nitrogen to phosphorus (N : P) ratios decrease with increasing growth rate. These results suggest that coccolithophores could reallocate chemical elements and energy to synthesize macromolecules efficiently, which allows them to regulate its elemental content and growth rate to acclimate to changing environmental conditions.

https://doi.org/10.5194/egusphere-2022-947
Preprint. Discussion started: 10 October 2022

1 Introduction

Continuous increase in atmospheric CO_2 level, as a consequence of anthropogenic activities, leads to global and ocean warming, which in turn shoals the ocean upper mixed layer (UML), hinders upward transport of nutrients from deeper ocean to the UML and increases light exposures to phytoplankton cells dwelling therein (Steinacher et al., 2010; Wang et al., 2015). The dissolution of CO_2 in the oceans is causing a significant chemical shift toward higher CO_2 and proton ($[H^+]$) concentrations, a process defined as ocean acidification (OA) (Caldeira and Wickett, 2003). These ocean changes expose phytoplankton cells within the UML to multiple drivers, and understanding the effects of changing multiple environmental drivers on the physiology and biochemistry of marine phytoplankton is important for projections of changes in the biogeochemical roles of phytoplankton in the future ocean (Gao et al., 2019).

Coccolithophores take up carbon dioxide (CO_2) to produce particulate organic carbon (POC) via photosynthesis, and use bicarbonate (HCO_3^-) and calcium (Ca^{2+}) to synthesize calcium carbonate plates (coccoliths, PIC) and release CO_2 via calcification, and play a critical role in the marine carbon cycle (Rost and Riebesell, 2004). The cosmopolitan coccolithophore *Emiliania huxleyi* typically forms extensive blooms that are easily detected by satellite remote sensing due to high light scattering caused by coccoliths (Terrats et al., 2020; He et al., 2022). Within *E. huxleyi* blooms in polar and subpolar oceans, dissolved nitrate and phosphate concentrations in surface seawater could be as lower as 0.95 μmol L^{-1} and 0.16 μmol L^{-1}, respectively (Townsend et al., 1994), light intensity are higher than 300 μmol photons m^{-2} s^{-1} (Tyrrell and Merico, 2004), and the mean concentrations of seawater CO_2 increased by 21.0%–43.3% which weakens the oceanic CO_2 uptake from the atmosphere

https://doi.org/10.5194/egusphere-2022-947
Preprint. Discussion started: 10 October 2022

(Kondrik et al., 2018). *Emiliania huxleyi* is also the dominant phytoplankton species in the lower photic zone in the north-eastern Caribbean Sea (western Atlantic Ocean) (Jordan and Winter, 2000) and in the South Pacific Gyre where dissolved nitrate and phosphate concentration are about 1.0 μmol L^{-1} and 0.2 μmol L^{-1}, respectively, and light intensity is lower than 20 μmol photons m^{-2} s^{-1} (Beaufort et al., 2008; Perrin et al., 2016). To explore how *E. huxleyi* acclimate to simultaneous changes in macronutrient concentration, light intensity and CO_2 level, it is interesting to investigate their physiological and biochemical processes, which can also help to project the effect of coccolithophores on ocean carbon cycle and ecological systems.

For more than a decade, research has shown that *E. huxleyi* cells developed several strategies to acclimate to reduced phosphorus availability, increasing light intensity and ocean acidification (Leonardos and Geider, 2005; McKew et al., 2015; Wang et al., 2022). Interactive effects of phosphorus availability and light intensity have shown that under phosphorus limitation condition, cells increased expression and the activity of alkaline phosphatase, and took up and used phosphorus efficiently under high light intensity, whereas they lowered the phosphorus uptake rate under low light intensity (Riegman et al., 2000; Perrin et al., 2016). In addition, the positive effect of reduced phosphorus availability on POC and PIC contents of *E. huxleyi* was further enhanced by increasing light intensity due to high-light-induced increases in CO_2 and HCO_3^- uptake rates under low phosphate availability (Leonardos and Geider, 2005). The negative effect of reduced phosphorus availability on particulate organic phosphorus (POP) content was partly compensated by increased PO_4^{3-} uptake rate under increasing light intensity (Perrin et al., 2016). On the other hand, several studies report that ocean acidification and reduced phosphorus availability acted synergistically to increase the POC content, especially at high light intensity, and

https://doi.org/10.5194/egusphere-2022-947
Preprint. Discussion started: 10 October 2022

acted antagonistically to affect PIC content of *E. huxleyi* (Leonardos and Geider, 2005; Matthiessen et al., 2012; Zhang et al., 2020). In addition, ocean acidification normally amplified the positive effect of increasing light intensity on POC content (Rokitta and Rost, 2012; Heidenreich et al., 2019). Due to high proton concentration-induced reduction in HCO_3^- uptake rate, ocean acidification could weaken or counteract the positive effect of increasing light intensity on PIC content (Rokitta and Rost, 2012; Kottmeier et al., 2016). Overall, while recent studies have focused on physiological performance of *E. huxleyi* and their effects on marine biogeochemical cycling of carbon, little information is available about the biochemical response of *E. huxleyi* to reduced phosphorus availability, increasing light intensity and ocean acidification.

The objective of this study is to investigate the combined effects of reduced phosphorus availability, increasing light intensity and ocean acidification on cellular elemental contents, the carbon (C) : nitrogen (N) : phosphorus (P) ratio and macromolecules of *E. huxleyi*, and to analyze the effects of macromolecules on elemental contents. Under reduced phosphorus availability, increasing light intensity and ocean acidification, we hypothesize that increased POC content is more likely to be caused by increased carbohydrate content. In addition, we discuss the potential mechanisms for changing PIC content in response to changed levels of phosphate, light, and CO_2, which is important for projections of changes in coccolithophore biogeochemistry and ecology in the future ocean.

2 Materials and Methods

2.1 Experimental setup

Emiliania huxleyi strain RCC1266 (morphotype A) was originally isolated from shelf waters around Ireland (49°30' N, 10°30' W) and obtained from the Roscoff algal

https://doi.org/10.5194/egusphere-2022-947
Preprint. Discussion started: 10 October 2022

culture collection. *Emiliania huxleyi* was cultured under a 14 h : 10 h light : dark cycle (light period: 06:00 to 20:00 h) in a thermo-controlled incubator (MGC-400H, Shanghai Yiheng Scientific Instrument) at 20ºC in semicontinuous cultures. The artifical seawater (ASW) media was prepared according to Berges et al. (2001) with the addition of 2350 μmol L^{-1} bicarbonate to achieve the total alkalinity (TA) of 2350 μmol L^{-1}, and enriched with 64 μmol L^{-1} NO_3^-, f/8 concentrations for trace metals and vitamins (Guillard and Ryther, 1962). The experiment was conducted in two parts (Fig. S1). The first part (Part 1) was performed at 40 μmol photons m^{-2} s^{-1} (low light intensity, LL) and the second one (Part 2) was at 300 μmol photons m^{-2} s^{-1} (high light intensity, HL). The LL intensity used here corresponds to the lower end of the irradiance range of the UML, and the HL intensity represents to the irradiance in the surface ocean (Jin et al., 2016; Perrin et al., 2016). For each part of the experiment, dissolved inorganic phosphorus (DIP) concentration and ocean acidification were combined in a fully factorial design: high DIP concentration (4 μmol L^{-1}) + low CO_2 level (426 μatm, current CO_2 level) (HP+LC, treatment 1 in LL and treatment 5 in HL), high DIP concentration (4 μmol L^{-1}) + high CO_2 level (946 μatm, future CO_2 level) (HP+HC, treatment 2 in LL and treatment 6 in HL), low DIP concentration (0.43 μmol L^{-1}) + low CO_2 level (426 μatm) (LP+LC, treatment 3 in LL and treatment 7 in HL), and low DIP concentration (0.43 μmol L^{-1}) + high CO_2 level (946 μatm) (LP+HC, treatment 4 in LL and treatment 8 in HL). High DIP concentration is replete for physiological process of *E. huxleyi*, and low DIP concentration corresponds to the upper end of the range of phosphate concentration in the coastal waters (Larsen et al., 2004). There were eight treatments totally and four biological replicates for each treatment (Fig. S1). In all cases, cell densities were lower than 78,000 cells mL^{-1} and the cells were acclimated to each treatment for at least 8 generations before

https://doi.org/10.5194/egusphere-2022-947
Preprint. Discussion started: 10 October 2022

physiological and biochemical parameters were measured.

At LL intensity (Part 1), for the treatments of HP+LC and HP+HC, the ASW media were enriched with 4 μmol L^{-1} PO_4^{3-} and aerated for 24 h at 20°C with filter-sterilized (PTFE filter, 0.22 μm pore size, Nantong) air pumped from the room. The pH_{Total} (total scale) values of the media under both HP+LC and HP+HC treatments were about 8.04. The dry air was humidified with Milli-Q water prior to the aeration to minimize evaporation. Under the HP+HC treatment, the pH_{Total} values of the media were adjusted to 7.74 by stepwise additions of CO_2-saturated seawater, and the ratio was about 6.5 mL CO_2-saturated seawater : 1000 mL ASW media. The CO_2-saturated seawater was achieved by bubbling pure CO_2 gas into 500 ml ASW media with a total alkalinity of 2350 μmol L^{-1} for 2 h. For the treatments of LP+LC and LP+HC, the ASW media were enriched with 0.4 μmol L^{-1} PO_4^{3-} and aerated for 24 h at 20°C with filtered room air. Under the LP+HC treatment, the pH_{Total} values of the media were also adjusted to 7.74 as described above. The HP+LC, HP+HC, LP+LC and LP+HC seawater were then filtered (0.22 μm pore size, Polycap 75 AS, Whatman) and carefully pumped into autoclaved 50 mL (for TA measurements), 600 mL (for pre-experimental cultures) and 2350 mL (for experimental cultures) polycarbonate bottles (Nalgene) with no headspace to minimize gas exchange. The volumes of culture inoculum were calculated to match the volumes of media taken out from the bottles prior to inoculation. The cells were inoculated to achieve an initial density of 5000 cells ml^{-1} in the HP+LC and HP+HC conditions, respectively, and cultured for 2 days, then diluted to the initial density again. These processes were performed three times in 600 mL bottles for pre-experimental cultures at 40 μmol photons m^{-2} s^{-1} (LL) of photosynthetically active radiation (PAR; measured using a LI-190SA quantum sensor, Beijing Ligaotai Technology Co. Ltd.). In the main experimental cultures in

https://doi.org/10.5194/egusphere-2022-947
Preprint. Discussion started: 10 October 2022

the HP+LC and HP+HC conditions at LL intensity, the cells were, respectively, transferred from 600 mL to 2350 mL bottles at the same time, and cultured for another 2 days (Fig. S1b). Culture bottles were rotated 10 times until cells were mixed at 09:00 h, 13:00 h and 19:00 h. Based on changes in cell densities during the incubations, we calculated that at LL intensity, cells were acclimated to HP+LC and HP+HC conditions for 10 generations. In the second day of the main experimental cultures, subsamples were taken for measurements of cell densities, pH_{Total}, TA, cellular contents of total particulate carbon (TPC), particulate organic carbon (POC), nitrogen (PON) and phosphorus (POP), carbohydrate and protein. At the end of the cultures under the previous conditions, cell samples with an initial density of 5000 cells ml^{-1} were transferred from HP+LC condition (treatment 1) to LP+LC condition (treatment 3), and from HP+HC condition (treatment 2) to LP+HC condition (treatment 4) at LL intensity. The cells were acclimated to LP+LC and LP+HC conditions for 8 generations before subsamples were taken for measurements.

At HL intensity (Part 2), samples grown under the HP+LC and HP+HC conditions were transferred from 40 (LL) to 300 µmol photons m^{-2} s^{-1} (HL) of PAR with initial cell density of 5000 cells ml^{-1}. The cells were cultured under the HP+LC and HP+HC conditions for 2 days, respectively, and then diluted back to the initial cell density. These processes were performed three times in 600 mL bottles at HL intensity, and then the main experimental cultures were conducted in 2350 mL bottles. The cells were, respectively, acclimated to HP+LC and HP+HC conditions for at least 8 generations at HL intensity. On the second day of the incubation, subsamples were taken for measurements of the parameters. After that, cell samples with an initial density of 5000 cells ml^{-1} were transferred from HP+LC condition (treatment 5) to LP+LC condition (treatment 7), and from HP+HC condition (treatment 6) to LP+HC

https://doi.org/10.5194/egusphere-2022-947
Preprint. Discussion started: 10 October 2022

condition (treatment 8). At HL intensity, cell samples were acclimated for at least 8 generations in LP+LC and LP+HC conditions, respectively, before subsamples were taken for measurements.

2.2 Phosphate concentration and carbonate chemistry measurements

In the beginning and on the second day of the incubations, samples for determinations of phosphate concentration (20 mL), pH_{Total} value (20 mL) and total alkalinity (TA) (50 mL) were, respectively, filtered (PTFE filter, 0.22 µm pore size, Nantong) 7 h after the onset of the light period (at 13:00). Dissolved inorganic phosphorus (DIP) concentration was measured using a spectrophotometer (SP-722, Shanghai Spectrum Instruments) following the phosphomolybdate method (Hansen and Koroleff, 1999). The bottle for pH measurement was filled from bottom to top with overflow and closed without a headspace. The pH_{Total} value was measured immediately at 20°C using a pH meter which was corrected with a standard buffer of defined pH in seawater (Dickson, 1993). TA samples were treated with 10 µL saturated $HgCl_2$ solution and stored in the dark at 4.0°C, and TA was measured at 20°C by potentiometric titration (AS-ALK1+, Apollo SciTech) according to Dickson et al. (2007). Carbonate chemistry parameters were estimated from TA and pH_{Total} using the CO2SYS program of Pierrot et al. (2006) with carbonic acid constants, K_1 and K_2, taken from Roy et al. (1993).

2.3 Cell density and elemental content measurements

Twenty milliliter samples to monitor the cell density were taken daily at 13:30 h, and fresh media with the same DIP concentration and carbonate chemistry as in the initial treatment conditions were added as top-up. Cell densities were determined using a

https://doi.org/10.5194/egusphere-2022-947
Preprint. Discussion started: 10 October 2022

Multisizer™3 Coulter Counter (Beckman Coulter). Growth rates were calculated for each replicate according to the equation: $\mu = (\ln N_t - \ln N_0) / d$, where N_t and N_0 refer to the cell densities on the second day and in the beginning of the main experiment, respectively, and d was the growth period in days.

After mixing, samples for determinations of TPC (300 mL), POC and PON (300 mL), and POP (300 mL) were obtained by filtering onto GF/F filters (precombusted at 450°C for 6 h) at the same time (14:00 h) in each treatment. For POC and PON measurements, samples were fumed with HCl for 12 h to remove inorganic carbon. TPC, POC and PON samples were dried at 60°C for 12 h and analyzed using an Elementar CHNS analyzer (Vario EL cube, GmbH, Germany). Cellular particulate inorganic carbon (PIC) content was calculated as the difference between cellular TPC and POC contents (Fabry and Balch, 2010). To remove dissolved inorganic phosphorus from the GF/F filters, POP samples were rinsed three times with 0.17 mol L^{-1} Na_2SO_4. After that, 2 mL 0.017 mol L^{-1} $MgSO_4$ solution was added onto filters, and POP samples were dried at 90°C for 12 h, and then combusted at 500°C for 6 h to remove POC and digested by 0.2 mol L^{-1} HCl (Solórzano and Sharp, 1980). Phosphorus concentration was measured using a microplate reader (Thermo Fisher) following the ammonium molybdate method (Chen et al., 1956) using adenosine-5-triphosphate disodium trihydrate as a standard.

2.4 Protein and carbohydrate measurements

Samples for determinations of protein (600 mL) and carbohydrate (600 mL) were, respectively, filtered onto polycarbonate filters (0.6 µm pore size, Nuclepore, Whatman) and onto precombusted GF/F filters at 14:30 h. Protein samples were extracted by bead milling (FastPrep Lysing Matrix D) in 0.5 mL 1× protein extraction

https://doi.org/10.5194/egusphere-2022-947
Preprint. Discussion started: 10 October 2022

buffer (lithium dodecyl sulfate, ethylene diamine tetraacetic acid, Tris, glycerol and 4-(2-aminoethyl) benzenesulfonyl fluoride hydrochloride). Bead milling was performed four times for 1 min at 6.5 ms^{-1}, and samples were placed on ice for 2 min between each round of bead milling to prevent degradation. The samples were then centrifuged at 10,000 × *g* for 5 min (Centrifuge 5418 R, Eppendorf, Germany), and extracted protein in the supernatant was quantified using the BCA assay with bovine gamma globulin as a standard using a microplate reader (Ni et al., 2016). Carbohydrate samples were hydrolyzed with 12.00 mol L^{-1} H_2SO_4 in the dark for 1 h and diluted by Milli-Q water to a final H_2SO_4 concentration of 1.20 mol L^{-1}. Then, samples were sonicated for 5 min, vortexed for 30 s, and boiled at 90°C for 3 h (Pakulski and Benner, 1992). The extracted carbohydrate was determined by phenol sulfuric reaction with D–glucose as standard (Masuko et al., 2005).

2.5 Data analysis

The percentages of carbon and nitrogen contributed by carbohydrate and protein were calculated from the elemental composition of biochemical classes compiled by Geider and LaRoche (2002). A three-way ANOVA was used to determine the main effects of DIP concentration, light intensity and CO_2 level, and their interactions on each variable. A Tukey post hoc test was performed to identify significant differences between two DIP concentrations, two light intensities and two CO_2 levels. A Shapiro–Wilk test was conducted to analyze the normality of residuals and a Levene test was conducted graphically to test for homogeneity of variances. All data analyses were conducted using the statistical software *R* with the packages carData, lattice and nlme (R version 3.5.0).

https://doi.org/10.5194/egusphere-2022-947
Preprint. Discussion started: 10 October 2022

3 Results

3.1 Dissolved inorganic phosphorus concentration and carbonate chemistry parameters

During the incubations, organismal activity significantly reduces dissolved inorganic phosphorus (DIP) concentrations (Table 1). Under high phosphorus (HP) treatment, DIP concentrations decrease by 20.32% in low light (LL) and low CO_2 (LC), by 22.32% in LL and high CO_2 (HC), by 27.66% in high light (HL) and LC, and by 31.58% in HL and HC. Under low phosphorus (LP) treatment, DIP concentrations decrease from 0.43 μmol L^{-1} at the beginning of the experiment to be lower than 0.04 μmol L^{-1} (the detection limit) at the end of the incubation in LL and LC conditions, in LL and HC conditions, in HL and LC conditions, and in HL and HC conditions.

During the incubations, at LL intensity, pH_T values increase by, on average, 0.02 in HP+LC, by 0.03 in HP+HC, by 0.09 in LP+LC, and by 0.10 in LP+HC conditions (Table 1). At HL intensity, pH_T values increase by 0.05 in HP+LC, by 0.06 in HP+HC, by 0.12 in LP+LC, and by 0.09 in LP+HC conditions. Correspondingly, at LL intensity, seawater CO_2 concentrations decrease by 5.53% in HP+LC, by 6.89% in HP+HC, by 22.76% in LP+LC, and by 22.77% in LP+HC. At HL intensity, seawater CO_2 concentrations decrease by 16.18% in HP+LC, by 16.41% in HP+HC, by 28.92% in LP+LC, and by 22.30% in LP+HC. Overall, organismal activity has larger effects on carbonate chemistry under the LP treatment than under the HP treatment.

3.2 Growth rate

The effect of increasing light intensity on growth rate is positive which can be seen by comparing growth rate in the HL regimes with their paired LL regimes (Fig. 1a,b; Table 2), though the extent of increase in growth rate depends on CO_2 levels and

https://doi.org/10.5194/egusphere-2022-947
Preprint. Discussion started: 10 October 2022

phosphate availability. Compared to LL intensity, growth rates at HL intensity increased by 48.48% in HP+LC, by 50.87% in HP+HC, by 60.86% in LP+LC, and by 60.80% in LP+HC (Tukey post hoc test, all values of $p < 0.01$). The effect of increasing CO_2 levels on growth rate depends on light intensity and phosphate availability (Fig. 1a,b). Compared to LC level, growth rates in HC level decreased by 3.08% in LL and HP condition ($p = 0.48$), by 16.13% in LL and LP condition ($p < 0.01$), by 1.50% in HL and HP condition ($p = 0.68$), and by 16.27% in HL and LP condition ($p < 0.01$). The effect of reduced phosphorus availability on growth rate is negative and the extent of reduction in growth rate depends on light intensity and CO_2 levels (Fig. 1a,b). Compared to HP availability, growth rates in LP availability decreased by 8.46% in LL and LC condition ($p <0.01$), by 20.81% in LL and HC condition ($p < 0.01$), by 0.76% in HL and LC condition ($p = 0.99$), and by 15.63% in HL and HC condition ($p < 0.01$). These results show that high CO_2 levels and low phosphorus availability acted synergistically to reduce growth rate of *E. huxleyi*, and increasing light intensity could partly counteract this response.

3.3 POC, PON, POP and PIC contents

The effect of increasing light intensity on POC content is positive, which was observed by comparing POC content in all the HL regimes with their paired LL regimes (Fig. 1c,d). The extent of increase in POC content depends on CO_2 levels and phosphate availability. Compared to LL intensity, POC contents at HL intensity increased by 27.15% in HP+LC, by 26.51% in HP+HC, by 43.24% in LP+LC, and by 58.13% in LP+HC conditions (Tukey post hoc test, all values of $p < 0.01$). The effect of increasing CO_2 levels on POC content is light and phosphate dependent and can be seen by comparing POC content in the HC regimes with their paired LC regimes (Fig.

https://doi.org/10.5194/egusphere-2022-947
Preprint. Discussion started: 10 October 2022

1c,d). At LL intensity, POC contents are not significantly different between HP+LC, HP+HC, LP+LC and LP+HC conditions (all values of $p > 0.1$). At HL intensity, compared to LC level, POC contents in HC level increased by 5.12% in HP condition ($p = 0.74$), and by 8.28% in LP condition ($p = 0.07$). The effect of phosphate reduction on POC content is light and CO_2 dependent, which can be seen by comparing POC content in the LP regimes with those in their paired HP regimes (Fig. 1c,d). At LL intensity, POC contents did not significantly differ between LP and HP availability. At HL intensity, compared to HP availability, POC contents in LP availability increased by 11.80% in LC condition ($p = 0.02$), and by 15.28% in HC condition ($p < 0.01$). These results show that ocean acidification and reduced phosphorus availability acted synergistically to increase POC contents in HL condition but not in LL condition.

The effect of increasing light intensity on PON content depends on CO_2 levels and phosphate availability (Fig. 1e,f). Compared to LL intensity, PON contents at HL intensity increased by 12.03% in HP+LC condition ($p = 0.27$), by 19.54% in HP+HC condition ($p < 0.01$), by 22.68% in LP+LC condition ($p < 0.01$), and by 30.90% in LP+HC condition ($p < 0.01$). The effect of increasing CO_2 levels on PON content is light and phosphate dependent, which can be seen by comparing POC content in the HC regimes with their paired LC regimes (Fig. 1e,f). Compared to LC level, PON contents in HC level did not change significantly in LL and HP condition, in LL and LP condition, in HL and LP condition, and increased by 14.68% in HL and HP condition ($p = 0.02$). The effect of phosphate reduction on PON content is CO_2 and light dependent, which can be seen by comparing PON content in the LP regimes with those in their paired HP regimes (Fig. 1e,f). Compared to HP availability, PON contents in LP availability decreased by 16.59% in LL and LC condition ($p = 0.01$),

https://doi.org/10.5194/egusphere-2022-947
Preprint. Discussion started: 10 October 2022

by 24.03% in LL and HC condition ($p < 0.01$), by 8.35% in HL and LC condition ($p = 0.43$), and by 17.32% in HL and HC condition ($p < 0.01$). These results show that increasing light intensity compensated for the negative effect of phosphate reduction on PON content.

The effect of increasing light intensity on POP content is positive and can be seen by comparing POP content in the HL regimes with their paired LL regimes, though the extent of increase in POP content depends on CO_2 levels and phosphate availability (Fig. 1g,h). Compared to LL intensity, POP contents at HL intensity increased by 35.79% in HP+LC, by 41.70% in HP+HC, by 57.22% in LP+LC, and by 56.44% in LP+HC conditions (Tukey post hoc test, all values of $p < 0.01$). Ocean acidification did not change the POP contents significantly in LL and HP condition, in LL and LP condition, in HL and HP condition, and in HL and LP condition (all values of $p > 0.53$) (Fig. 1g,h). Reduced phosphorus availability significantly decreased the POP contents, which can be seen by comparing POP content in the LP regimes with their paired HP regimes, though the extent of reduction in POP content depends on light intensity and CO_2 levels (Fig. 1g,h). Compared to HP availability, POP contents in LP availability decreased by 52.96% in LL and LC condition, by 54.03% in LL and HC condition, by 46.11% in HL and LC condition, and by 49.51% in HL and HC condition (all values of $p < 0.01$). These results show that reduced phosphorus availability had a larger effect on POP content than that of ocean acidification and increasing light intensity.

The effect of increasing light intensity on PIC content is positive, which can be seen by comparing PIC content in the HL regimes with their paired LL regimes, though the extent of increase in PIC content depends on CO_2 levels and phosphorus availability (Fig. 1i,j). Compared to LL intensity, PIC contents at HL intensity

https://doi.org/10.5194/egusphere-2022-947
Preprint. Discussion started: 10 October 2022

increased by 77.87% in HP+LC, by 70.28% in HP+HC, by 98.31% in LP+LC, and by 90.68% in LP+HC conditions (Tukey post hoc test, all values of $p < 0.01$). The effect of increasing CO_2 levels on PIC content is negative and can be seen by comparing PIC content in the HC regimes with those in their paired LC regimes (Fig. 1i,j). The extent of reduction in PIC content depends on light intensity and phosphorus availability. Compared to LC level, PIC contents under ocean acidification decreased by 31.43% in LL and HP condition ($p = 0.09$), by 16.00% in LL and LP condition ($p = 0.67$), by 35.02% in HL and HP condition ($p < 0.01$), and by 21.12% in HL and LP condition ($p < 0.01$). The effect of phosphate reduction on PIC content is positive which can be seen by comparing PIC content in the LP regimes with their paired HP regimes, though the extent of increase in PIC content depends on light intensity and CO_2 levels (Fig. 1i,j). Compared to HP availability, PIC contents in LP availability increased by 16.00% in LL and LC condition ($p = 0.83$), by 41.26% in LL and HC condition ($p = 0.16$), by 29.98% in HL and LC condition ($p < 0.01$), and by 60.44% in HL and HC condition ($p < 0.01$). These results show that high light intensity and low phosphorus availability acted synergistically to increase PIC content, which counteracts the negative effect of ocean acidification on PIC content.

3.4 Carbohydrate and protein contents

The effect of increasing light intensity on carbohydrate content is positive and can be seen by comparing carbohydrate content in the HL regimes with their paired LL regimes, though the extent of increase in carbohydrate depends on CO_2 levels and phosphorus availability (Fig. 2a,b). Compared to LL intensity, cellular carbohydrate contents at HL intensity increased by 148.81% in HP+LC condition, by 139.42% in HP+HC condition, by 179.12% in LP+LC condition, and by 204.42% in LP+HC

https://doi.org/10.5194/egusphere-2022-947
Preprint. Discussion started: 10 October 2022

condition (all values of $p < 0.01$). The effect of increasing CO_2 levels on carbohydrate content is light and phosphate dependent which can be seen by comparing carbohydrate content in the HC regimes with their paired LC regimes (Fig. 2a,b). Compared to LC level, carbohydrate contents under ocean acidification increased by 26.55% in LL and HP condition ($p = 0.58$), by 8.91% in LL and LP condition ($p = 0.99$), by 21.32% in HL and HP condition ($p = 0.02$), and by 18.45% in HL and LP condition ($p < 0.01$). The effect of phosphate reduction on carbohydrate content is light and CO_2 dependent and can be seen by comparing carbohydrate content in the LP regimes with their paired HP regimes (Fig. 2a,b). Compared to HP availability, carbohydrate contents in LP availability did not change significantly in LL and LC condition, in LL and HC condition (both $p > 0.65$) and increased by 40.13% in HL and LC condition ($p < 0.01$), and by 36.00% in HL and HC condition ($p < 0.01$). These results show that increasing light intensity dominantly increased carbohydrate content, and ocean acidification and reduced phosphorus availability acted synergistically to increase carbohydrate contents under high light intensity.

The effect of increasing light intensity on protein content is positive, which can be seen by comparing protein content in the HL regimes with their paired LL regimes, though the extent of increase in protein content depends on CO_2 level and phosphorus availability (Fig. 2c,d). Compared to LL intensity, protein contents at HL intensity increased by 24.76% in HP+LC condition, by 30.43% in HP+HC condition, by 68.09% in LP+LC condition, and by 65.39% in LP+HC condition (all values of $p < 0.01$). The effect of increasing CO_2 levels on protein content can be seen by comparing protein content in the HC regimes with their paired LC regimes (Fig. 2c,d). Compared to LC level, protein contents under ocean acidification did not change significantly in LL and HP condition, in LL and LP condition, in HL and HP

https://doi.org/10.5194/egusphere-2022-947
Preprint. Discussion started: 10 October 2022

condition, and in HL and LP condition (all values of $p > 0.09$). The effect of phosphate reduction on protein content is light and CO_2 dependent, which can be seen by comparing protein content in the LP regimes with their paired HP regimes (Fig. 2c,d). Compared to HP availability, protein content in LP availability decreased by 27.88% in LL and LC condition, by 28.80% in LL and HC condition (both $p < 0.01$) and did not change significantly in HL and LC condition, and in HL and HC condition (both $p > 0.11$). These results show that high light intensity counteracted the negative effect of low phosphorus availability on protein content, and ocean acidification had less effect on protein content.

3.5 Percentage of POC allocated to carbohydrate (carbohydrate–C : POC) and protein (protein–C : POC)

Increasing light intensity increased the percentage of POC allocated to carbohydrate (carbohydrate–C : POC), which can be seen by comparing carbohydrate–C : POC in the HL regimes with their paired LL regimes, though the extent of increase in carbohydrate–C : POC depends on CO_2 levels and phosphorus availability (Fig. 2e,f). Compared to LL intensity, carbohydrate–C : POC at HL intensity increased by 95.60% in HP+LC condition, by 97.69% in HP+HC condition, by 95.05% in LP+LC condition, and by 83.37% in LP+HC condition (all values of $p < 0.01$). The effect of increasing CO_2 levels on carbohydrate–C : POC is light and phosphate dependent, and can be seen by comparing carbohydrate–C : POC in the HC regimes with their paired LC regimes (Fig. 2e,f). Compared to LC level, carbohydrate–C : POC under ocean acidification increased by 20.12% in LL and HP condition, by 11.42% in LL and LP condition, by 20.36% in HL and HP condition, and by 4.40% in HL and LP condition (all values of $p > 0.08$). The effect of phosphate reduction on carbohydrate–C : POC

https://doi.org/10.5194/egusphere-2022-947
Preprint. Discussion started: 10 October 2022

is light and CO_2 dependent, which can be seen by comparing carbohydrate–C : POC in the LP regimes with those in their paired HP regimes (Fig. 2e,f). Compared to HP availability, carbohydrate–C : POC in LP availability increased by 25.61% in LL and LC condition ($p = 0.16$), by 17.37% in LL and HC condition ($p = 0.47$), by 25.81% in HL and LC condition ($p < 0.01$), and by 8.11% in HL and HC condition ($p < 0.05$). These results show that increasing light intensity, ocean acidification and reduced phosphorus availability acted synergistically to increase the percentage of POC allocated to carbohydrate.

Increasing light intensity did not significantly change the percentage of POC allocated to protein (protein–C : POC) in HP+LC, HP+HC, LP+LC and LP+HC conditions (Fig. 2g,h). Ocean acidification did not significantly affect the protein–C : POC in LL and HP, in LL and LP, in HL and HP, and in HL and LP conditions. The effect of phosphate reduction on protein–C : POC is light and CO_2 dependent, which can be seen by comparing the protein–C : POC in the LP regimes with their paired HP regimes (Fig. 2g,h). Compared to HP availability, protein–C : POC in LP availability decreased by 27.39% in LL and LC condition ($p < 0.01$), by 23.05% in LL and HC condition ($p < 0.01$), by 12.81% in HL and LC condition ($p = 0.09$), and by 21.77% in HL and HC condition ($p < 0.01$). These results show that reduced phosphorus availability dominantly reduced the protein–C : POC, and increasing light intensity and ocean acidification had less effects on protein–C : POC.

3.6 Elemental stoichiometry and protein content as a function of growth rate

At LL and HL intensities, both POC : POP ratio and PON : POP ratio were linearly and negatively correlated with growth rates (Fig. 3a,b). In LL and HL conditions, POC : POP ratio decreased linearly with increasing growth rate ($R^2 = 0.71$, $F = 32.08$,

https://doi.org/10.5194/egusphere-2022-947
Preprint. Discussion started: 10 October 2022

$p < 0.01$ in LL condition; $R^2 = 0.53$, $F = 14.63$, $p < 0.01$ in HL condition). Similarly, in LL and HL conditions, PON : POP ratio decreased linearly with increasing growth rate ($R^2 = 0.69$, $F = 29.23$, $p < 0.01$ in LL condition; $R^2 = 0.50$, $F = 13.31$, $p < 0.01$ in HL condition). In all treatments, protein content increased linearly with increasing growth rate ($R^2 = 0.76$, $F = 151.14$, $p < 0.01$) (Fig. 3c), and POC content increased linearly with increasing carbohydrate content ($R^2 = 0.94$, $F = 435.10$, $p < 0.01$) (Fig. 3d).

4 Discussion

Coccolithophores make an important contribution to marine biological carbon pump and their responses to global climate change could have significant consequences for marine carbon cycling (Riebesell et al., 2017). The bloom-forming coccolithophore *E. huxleyi*, dominating the assemblages in seawater under limited phosphorus condition, is likely to be exposed to increasing light intensity and ocean acidification in the future ocean (Kubryakova et al., 2021). In this study, we observed that increasing light intensity compensates for the negative effects of low phosphorus availability on cellular protein and nitrogen contents (Figs. 1 and 2). Reduced phosphorus availability, increasing light intensity and ocean acidification act synergistically to increase cellular contents of carbohydrate and POC, and the allocation of POC to carbohydrate. These regulation mechanisms in *E. huxleyi* could provide vital information for evaluating carbon cycle in marine ecosystems under global change.

Ribonucleic acid (RNA) is the main phosphorus-containing macromolecule within the cell (Geider and La Roche, 2002). Therefore, the reduced phosphorus availability dominantly reduces the RNA content (Fig. S5), which contributes to low POP contents (McKew et al., 2015) (Fig. 1g,h). In eukaryotic cells, ribosomal RNA (rRNA)

https://doi.org/10.5194/egusphere-2022-947
Preprint. Discussion started: 10 October 2022

constitutes about 80% of the total RNA and is mainly used to create ribosome (Dyhrman, 2016). Thus, reduced RNA contents decrease the numbers of ribosome, which has a potential to decrease protein synthesis (Dyhrman, 2016; Rokitta et al., 2016). On the other hand, low light intensity reduces the nitrate uptake and assimilation efficiency of *E. huxleyi* and other phytoplankton species (Perrin et al., 2016; Lu et al., 2018), which exacerbates the negative effect of low phosphorus availability on protein synthesis and PON contents (Figs. 1e and 2c). Besides that, low light intensity significantly reduces the rates of RNA synthesis, carbohydrate synthesis and cell division (Zhang et al., 2021), which adds to the negative effect of low phosphorus availability on growth rate of *E. huxleyi* (Fig. 1a). Under high light intensity and low CO_2 level, reduced phosphorus availability did not change growth rate and protein content (Figs. 1b and 2d), which suggests that *E. huxleyi* might compensate for low phosphate-induced decreases in ribosome content by increasing protein synthesis efficiency under increasing light intensity (Reith and Cattolico, 1985). Under high light intensity and ocean acidification, reduced phosphorus availability did not significantly change protein content while reduced growth rate, which might indicate the lowered protein synthesis efficiency (McKew et al., 2015).

Several studies report that reduced phosphorus availability (0.4–0.5 μmol L^{-1}) did not change growth rates significantly during the short-time (2 or 3 days) incubations under low CO_2 level and high light intensity (Rokitta et al., 2016; Zhang et al., 2020; Wang et al., 2022) (Fig. S6). The reasons could be that *E. huxleyi* cells developed high affinity for phosphate and increased the uptake rate of phosphate (Wang et al., 2022) and could replace the phospholipid membrane with non-phosphorus membrane during the short-time incubation of phosphorus limitation (Shemi et al., 2016). Our data showed that reduced phosphorus availability and ocean acidification acted

https://doi.org/10.5194/egusphere-2022-947
Preprint. Discussion started: 10 October 2022

synergistically to reduce growth rate under both low and high light intensities (Fig. 1a,b). One of the reasons could be that low pH value under ocean acidification up regulates the expressions of a series of genes involved in ribosome metabolism, such as genes of large subunit ribosomal protein L3, L38E, L30E (*RP-L3*, *RP-L38E*, *RP-L30E*), and small subunit ribosomal protein S3E, S5E, SAE (*PR-S3E*, *PR-S5E*, *RP-SAE*) in *E. huxleyi* (Fig. S7). Under ocean acidification, up regulation of expression of these genes has the potential to drive cells to allocate more phosphorus to synthesize ribosome, and to reduce the allocation of phosphorus to DNA replication (Rokitta et al., 2011), which exacerbates the limitation of reduced phosphorus availability on the rate of cell division in *E. huxleyi* (Rouco et al., 2013). Under phosphorus-replete condition, more phosphorus is reallocated to ribosome metabolism under ocean acidification which could facilitate nitrogen assimilation (Fig. 2d). Overall, under high light intensity, ocean acidification is likely to facilitate *E. huxleyi* cells to increase nitrogen content in phosphorus-replete condition and to reduce growth rate in phosphorus-limitation.

In this study, we found that low light intensity dominantly limits carbon assimilation of *E. huxleyi* and reduces the effects of phosphate availability and ocean acidification on carbohydrate and POC contents (Figs. 1c and 2a). However, under high light intensity, *E. huxleyi* had high carbohydrate and POC contents while low growth rate under reduced phosphorus availability and ocean acidification (Figs. 1b,d and 2b), which suggests that carbon assimilation rate did not change significantly while cell division rate decreased (Matthiessen et al., 2012; Perrin et al., 2016). Furthermore, carbohydrate is a carbon- and energy-storing macromolecule (Geider and La Roche, 2002). Under high light intensity, reduced phosphorus availability and ocean acidification, *E. huxleyi* cells could synthesize more carbohydrate to store

https://doi.org/10.5194/egusphere-2022-947
Preprint. Discussion started: 10 October 2022

carbon and energy, which contributes to the large percentage of POC allocated to carbohydrate (Fig. 2f).

The physiological reasons for reduced calcification rate under ocean acidification could be due to high proton concentration-induced reduction in HCO_3^- uptake rate (Meyer and Riebesell, 2015; Kottmeier et al., 2016). The molecular mechanisms for low PIC content under ocean acidification may be due to down-regulation of a series of genes potentially involved in ion transport and pH regulation, such as genes of calcium/proton exchanger (*CAX3*), sodium/proton exchanger (*NhaA2*) and membrane-associated proton pump (*PATP*) (Mackinder et al., 2011; Lohbeck et al., 2014). On the other hand, increasing light intensity up-regulates a series of genes related to ion transport, such as gene of *CAX3*, gene of Cl^-/HCO_3^- exchanger and genes of various subunits of a vacuolar H^+–ATPase (*V–ATPase*) and so on (Rokitta et al., 2011). Up-regulation of these genes in high light intensity has the potential to facilitate cells to take up HCO_3^- and Ca^{2+}, and to pump proton outside the cells, and then leads to large PIC content of *E. huxleyi* (Kottmeier et al., 2016). Our data suggest that increasing light intensity counteracts the negative effect of ocean acidification on PIC content of *E. huxleyi* (Fig. 1i,j). These results are consistent with the findings of Feng et al. (2020) who reported that combinations of increasing light intensity and ocean acidification increase the expression of genes involved in calcium-binding proteins (*CAM* and *GPA*), which has the potential to increase calcium influx into cells and then compensate for the effect of reduced HCO_3^- uptake rate on calcification. It is also suggested that increasing light intensity could cause cells to remove H^+ faster which neutralizes the effect of high proton concentration on calcification (Jin et al., 2017). On the other hand, reduced phosphorus availability extends the G1 phase of cell cycle where calcification occurs, which prolongs the calcification time and then

https://doi.org/10.5194/egusphere-2022-947
Preprint. Discussion started: 10 October 2022

increases PIC content (Müller et al., 2008). In addition, reduced phosphorus availability up-regulates expressions of genes of Ca^{2+} uptake, proton removal and carbonic anhydrase, and then increases coccolith production (Wang et al., 2022), which contribute to a larger PIC content and counteract the negative effect of ocean acidification on PIC contents (Borchard et al., 2011) (Fig. 1i,j). Furthermore, one of the reasons for larger PIC contents under reduced phosphorus availability and increasing light intensity conditions are likely due to larger and more numerous coccoliths (Gibbs et al., 2013; Perrin et al., 2016). Overall, responses of calcification of *E. huxleyi* to ocean climate change are complex than previously thought (Meyer and Riebesell, 2015), and it is worth exploring the underlying mechanisms of calcification under changing multiple environmental drivers (Mackinder et al., 2011; Feng et al., 2020).

Cellular POP content of *E. huxleyi* generally decreased, and POC : POP ratio and PON : POP ratio increased with reducing phosphorus availability (Leonardo and Geider, 2005; McKew et al., 2015). The negative correlations between growth rate and POC : POP ratio or PON : POP ratio under each light intensity are consistent with the growth rate hypothesis (Fig. 3), which proposes that growth rate increases with increasing RNA : protein ratio. Phosphorus in RNA accounts for a high percentage of total POP, whereas nitrogen in protein is the main form of PON (Zhang et al., 2021), and the growth rate hypothesis suggests that growth rate could increase with decreasing POC : POP ratio or PON : POP ratio (Sterner and Elser, 2002). Our results suggest that *E. huxleyi* could reallocate chemical elements and energy to synthesize carbohydrate, protein and RNA efficiently, and then regulate its elemental stoichiometry and growth rate to acclimate to reduced phosphorus availability, ocean acidification and increasing light intensity (Moreno and Martiny, 2018). In the future

https://doi.org/10.5194/egusphere-2022-947
Preprint. Discussion started: 10 October 2022

ocean, large carbohydrate and POC contents, POC : PON ratio, and POC : POP ratio of coccolithophores indicate increases in carbon export to the deep ocean that may affect the efficiency of the biological carbon pump and the marine biogeochemical cycle of carbon.

Data availability. The data are available upon request to the corresponding author (yongzhang@fjnu.edu.cn).

Author contributions. YZ (yongzhang@fjnu.edu.cn), ZL and KX contributed to the design of the experiment. YZ (yongzhang@fjnu.edu.cn), YZ (qsx20211022@student.fjnu.edu.cn), SM, HC and RH performed this experiment and biochemical analyses. YZ (yongzhang@fjnu.edu.cn) wrote the first manuscript draft. All authors contributed to the data analyses and editing of the paper.

Competing interests. The authors declare that they have no conflict of interest.

Acknowledgments. We would like to thank Professor Zoe V. Finkel for providing the *Emiliania huxleyi* RCC1266, Dr. Vinitha Ebenezer for her helpful revision of the manuscript and two reviewers for their helpful suggestions which have help us to improve the manuscript. This work was supported by the National Natural Science Foundation of China (41806129 [YZ], 32001180 [ZKL]).

https://doi.org/10.5194/egusphere-2022-947
Preprint. Discussion started: 10 October 2022

References

Beaufort, L., Couapel, M., Buchet, N., Claustre, H., and Goyet, C.: Calcite production by coccolithophores in the southeast Pacific Ocean, Biogeosciences, 5, 1101–1117, doi:10.5194/bg-5-1101-2008, 2008.

Berges, J. A., Franklin, D. J., and Harrison, P. J.: Evolution of an artificial seawater medium: improvements in enriched seawater, artificial water over the past two decades, J. Phycol., 37, 1138–1145, doi: 10.1046/j.1529-8817.2001.01052.x, 2001.

Borchard, C., Borges, A. V., Händel, N., and Engel, A.: Biogeochemical response of *Emiliania huxleyi* (PML B92/11) to elevated CO_2 and temperature under phosphorus limitation: A chemostat study, J. Exp. Mar. Biol. Ecol., 410, 61–71, doi: 10.1016/j.jembe.2011.10.004, 2011.

Caldeira, K., and Wickett, M. E.: Oceanography: anthropogenic carbon and ocean pH, Nature, 425, 365, doi: 10.1038/425365a, 2003.

Chen, P., Toribara, T. T., and Warner, H.: Microdetermination of phosphorus, Anal. Chem., 28, 1756–1758, doi: 10.1021/ac60068a036, 1956.

Dickson, A. G., Sabine, C. L., and Christian, J. R.: Guide to best practice for ocean CO_2 measurements, PICES Special Publication 3, pp. 191, 2007.

Dickson, A. G.: pH buffers for seawater media based on the total hydrogen ion concentration scale, Deep-Sea Res., 40, 107–118, doi: 10.1016/0967-0637(93)90055-8, 1993.

Dyhrman, S. T.: Nutrients and their acquisition: phosphorus physiology in microalgae, in: The physiology of microalgae, edited by: Borowitzka, M. A., Beardall, J. and Raven, J. A., Springer, Heidelberg, 155–183, doi: 10.1007/978-3-319-24945-2, 2016.

https://doi.org/10.5194/egusphere-2022-947
Preprint. Discussion started: 10 October 2022

Fabry, V. J., and Balch, W. M.: Direct measurements of calcification rates in planktonic organisms, in: Guide to best practices for ocean acidification research and data reporting, edited by: Riebesell, U., Fabry, V. J., Hansson, L. and Gattuso, J. P., Luxembourg, Publications Office of the European Union, p. 201–212, doi: 10.2777/66906, 2010.

Feng, Y. Y., Roleda, M. Y., Armstrong, E., Summerfield, T. C., Law, C. S., Hurd, C. L., and Boyd, P. W.: Effects of multiple drivers of ocean global change on the physiology and functional gene expression of the coccolithophore *Emiliania huxleyi*, Glob. Chang. Biol., 26, 5630–5645, doi: 10.1111/GCB.15259, 2020.

Gao, K., Beardall, J., Häder, D. P., Hall-Spencer, J. M., Gao, G., and Hutchins, D. A.: Effects of ocean acidification on marine photosynthetic organisms under the concurrent influences of warming, UV radiation, and deoxygenation, Front. Mar. Sci., 6, 322, https://doi.org/10.3389/fmars.2019.00322, 2019.

Geider, R. J., and LaRoche, J.: Redfield revisited: variability of C:N:P in marine microalgae and its biochemical basis, Eur. J. Phycol., 37, 1–17, doi: 10.1017/S0967026201003456, 2002.

Gibbs, S. J., Poulton, A. J., Brown, P. R., Daniels, C. J., Hopkins, J., Young, J. R., Jones, H. L., Thiemann, G. J., O'Dea, S. A., and Newsam, C.: Species-specific growth response of coccolithophores to Palaeocene – Eocene environmental change, Nat. Geosci., 6, 218–222, doi: 10.1038/ngeo1719, 2013.

Guillard, R. R. L., and Ryther, J. H.: Studies of marine planktonic diatoms. I. Cyclotella nana Hustedt and Detonula confervacea Cleve, Can. J. Microbiol., 8, 229–239, doi: 10.1139/m62-029, 1962.

Hansen, H. P., and Koroleff, F.: Determination of nutrients, in: Methods of seawater analysis, edited by: Grasshoff, K., Kremling, K. and Ehrhardt, M., WILEY-VCH

https://doi.org/10.5194/egusphere-2022-947
Preprint. Discussion started: 10 October 2022

Publishers, ISBN: 3-527-29589-5, 1999.

He, S., Le, C., He, J., and Liu, N.: Empirical algorithm for detecting coccolithophore blooms through satellite observation in the Barents Sea, Remote Sens. Environ., 270, 112886, doi: 10.1016/j.res.2021.112886, 2022.

Heidenreich, E., Wördenweber, R., Kirschhöfer, F., Nusser, M., Friedrich, F., Fahl, K., Kruse, O., Rost, B., Franzreb, M., Brenner-Weiß, G., and Rokitta, S.: Ocean acidification has little effect on the biochemical composition of the coccolithophore *Emiliania huxleyi*, PLoS One, 14, e0218564, doi: 10.1371/journal.pone.0218564, 2019.

Jin, P., Gao, G., Liu, X., Li, F., Tong, S., Ding, J., Zhong, Z., Liu,N., and Gao, K.: Contrasting photophysiological characteristics of phytoplankton assemblages in the Northern South China Sea, PLoS ONE, 11, e0153555, doi: 10.1371/journal.pone.0153555, 2016.

Jin, P., Ding, J. C., Xing, T., Riebesell, U., and Gao, K. S.: High levels of solar radiation offset impacts of ocean acidification on calcifying and non-calcifying strains of *Emiliania huxleyi*, Mar. Ecol. Prog. Ser., 568, 47–58, doi: 10.3354/meps12042, 2017.

Jordan, R. W., and Winter, A: Assemblages of coccolithophorids and other living microplankton off the coast of Puerto Rico during January–May 1995, Mar. Micropaleontol., 39, 113–130, doi: 10.1016/S0377-8398(00)00017-7, 2000.

Kondrik, D. V., Pozdnyakov, D. V., and Johannessen, O. M.: Satellite evidence that *E. huxleyi* phytoplankton blooms weaken marine carbon sinks, Geophys. Res. Lett., 45, e2017GL076240, doi: 10.1002/2017GL076240, 2018.

Kottmeier, D. M., Rokitta, S. D., and Rost, B.: Acidification, not carbonation, is the major regulator of carbon fluxes in the coccolithophore *Emiliania huxleyi*, New

https://doi.org/10.5194/egusphere-2022-947
Preprint. Discussion started: 10 October 2022

Phytol., 211, 126–137, doi: 10.1111/nph.13885, 2016.

Kubryakova, E. A., Kubryakov, A. A., and Mikaelyan, A. S.: Winter coccolithophore blooms in the Black Sea: Interannual variability and driving factors, J. Mar. Syst., 213, 103461, doi: 10.1016/j.jmarsys.2020.103461, 2021.

Larsen, A., Flaten, G. A. F., Sandaa, R., Castberg, T., Thyrhaug, R., Erga, S. R., Jacquet, S., and Bratbak, G.: Spring phytoplankton bloom dynamics in Norwegian coastal waters: Microbial community succession and diversity, Limnol. Oceanogr., 49, 180–190, doi: 10.4319/lo.2004.49.1.0180, 2004.

Leonardos, K., and Geider, R. J.: Elevated atmospheric carbon dioxide increases organic carbon fixation by *Emiliania huxleyi* (haptophyta), under nutrient-limited high-light conditions, J. Phycol., 41, 1196–1203, doi: 10.1111/j.1529-8817.2005.00152.x, 2005.

Lohbeck, K., Riebesell, U., and Reusch, T. B. H.: Gene expression changes in the coccolithophore *Emiliania huxleyi* after 500 generation of selection to ocean acidification, Proc. R. Soc. B., 281, 20140003, doi: 10.1098/rspb.2014.0003, 2014.

Lu, Y., Wen, Z., Shi, D., Chen, M., Zhang, Y., Bonnet, S., Li, Y., Tian, J., and Kao, S. J.: Effect of light on N_2 fixation and net nitrogen release of *Trichodesmium* in a field study, Biogeosciences, 15, 1–12, doi: 10.5194/bg-15-1-2018, 2018.

Mackinder, L., Wheeler, G., Schroeder, D., von Dassow, P., Riebesell, U., and Brownlee, C.: Expression of biomineralization-related ion transport genes in *Emiliania huxleyi*, Env. Microbiol., 13, 3250–3565, doi:10.1111/j.1462-2920.2011.02561.x, 2011.

Masuko, T., Minami, A., Iwasaki, N., Majima, T., Nishimura, S. I., and Lee, Y. C.: Carbohydrate analysis by a phenol-sulfuric acid method in microplate format,

https://doi.org/10.5194/egusphere-2022-947
Preprint. Discussion started: 10 October 2022

751 Anal. Biochem., 339, 69–72, doi: 10.1016/j.ab.2004.12.001, 2005.
752 Matthiessen, B., Eggers, S. L., and Krug, S. A.: High nitrate to phosphorus regime
753 attenuates negative effects of rising pCO_2 on total population carbon
754 accumulation, Biogeosciences, 9, 1195–1203, doi: 10.5194/bg-9-1195-2012,
755 2012.
756 McKew, B. A., Metodieva, G., Raines, C. A., Metodiev, M. V., and Geider, R. J.:
757 Acclimation of *Emiliania huxleyi* (1516) to nutrient limitation involves precise
758 modification of the proteome to scavenge alternative sources of N and P,
759 Environ. Microbiol., 17, 4050–4062, doi: 10.1111/1462-2920.12957, 2015.
760 Meyer, J., and Riebesell, U.: Reviews and syntheses: responses of coccolithophores to
761 ocean acidification: a meta-analysis, Biogeosciences, 12, 1671–1682, doi:
762 10.5194/bg-12-1671-2015, 2015.
763 Moreno, A. R., and Martiny, A. C.: Ecological stoichiometry of ocean plankton, Ann.
764 Rev. Mar. Sci., 10, 43–69, doi: 10.1146/annurev-marine-121916-063126, 2018.
765 Müller, M. N., Antia, A. N., and LaRoche, J.: Influence of cell cycle phase on
766 calcification in the coccolithophore *Emiliania huxleyi*, Limnol. Oceanogr., 53,
767 506–512, doi: 10.4319/lo.2008.53.2.0506, 2008.
768 Ni, G., Zimbalatti, G., Murphy, C. D., Barnett, A. B., Arsenault, C. M., Li, G.,
769 Cockshutt, A. M., and Campbell, D. A.: Arctic *Micromonas* uses protein pools
770 and non-photochemical quenching to cope with temperature restrictions on
771 Photosystem II protein turnover, Photosynth. Res., 131, 203–220, doi:
772 10.1007/s11120-016-0310-6, 2016.
773 Pakulski, J. D., and Benner, R.: An improved method for the hydrolysis and MBTH
774 analysis of dissolved and particulate carbohydrates in seawater, Mar. Chem., 40,
775 143–160, doi: 10.1016/0304-4203(92)90020-B, 1992.

https://doi.org/10.5194/egusphere-2022-947
Preprint. Discussion started: 10 October 2022

776 Perrin, L., Probert, I., Langer, G., and Aloisi, G.: Growth of the coccolithophore
777 *Emiliania huxleyi* in light- and nutrient-limited batch reactors: relevance for the
778 BIOSOPE deep ecological niche of coccolithophores, Biogeosciences, 13, 5983–
779 6001, doi: 10.5194/bg-13-5983-2016, 2016.
780 Pierrot, D., Lewis, E., and Wallace, D. W. R.: MS Excel program developed for CO_2
781 system calculations, ORNL/CDIAC-105, Carbon Dioxide Information Analysis
782 Centre, Oak Ridge National Laboratory, U.S., Department of Energy, doi:
783 10.3334/CDIAC/otg.CO2SYS_XLS_CDIAC105a, 2006.
784 R version 3.5.0.: The R foundation for statistical computing platform,
785 x86_64-w64-mingw32/x64. Available from:
786 https://cran.r-project.org/bin/windows/ base/old/3.5.0, 2018.
787 Reith, M. E., and Cattolico, R. A.: Chloroplast protein synthesis in the chromophytic
788 alga *Olisthodiscus luteus*, Plant Physiol., 79, 231–236, doi: 10.1104/pp.79.1.231,
789 1985.
790 Riebesell, U., Bach, L. T., Bellerby, R. G. J., Rafael Bermúdez Monsalve, J.,
791 Boxhammer, T., Czerny, J., Larsen, A., Ludwig, A., and Schulz, K. G.:
792 Competitive fitness of a predominant pelagic calcifier impaired by ocean
793 acidification, Nat. Geosci., 10, 19–24, dio: 10.1038/NGEO2854, 2017.
794 Riegman, R., Stolte, W., Noordeloos, A. A. M., and Slezak, D.: Nutrient uptake and
795 alkaline phosphatase (EC 3:1:3:1) activity of *Emiliania huxleyi*
796 (Prymnesiophyceae) during growth under N and P limitation in continuous
797 cultures, J. Phycol., 36, 87–96, 2000.
798 Rokitta, S. D., von Dassow, P., Rost, B., and John, U.: P- and N-depletion trigger
799 similar cellular responses to promote senescence in eukaryotic phytoplankton,
800 Front. Mar. Sci., 3, 109, doi: 10.3389/fmars.2016.00109, 2016

https://doi.org/10.5194/egusphere-2022-947
Preprint. Discussion started: 10 October 2022

Rokitta, S. D., and Rost, B: Effects of CO_2 and their modulation by light in the life-cycle stages of the coccolithophore *Emiliania huxleyi*, Limnol. Oceanog., 57, 607–618, doi: 10.4319/lo.2012.57.2.0607, 2012.

Rokitta, S. D., de Nooijer, L. J., Trimborn, S., de Vargas, C., Rost, B., and John, U.: Transcriptome analyses reveal differential gene expression patterns between the life-cycle stages of *Emiliania huxleyi* (haptophyta) and reflect specialization to different ecological niches, J. Phycol., 47, 829–838, doi: 10.1016/S0924-9338(02)00624-7, 2011.

Rost, B., and Riebesell, U.: Coccolithophores and the biological pump: responses to environmental changes, in: Coccolithophores : from molecular biology to global impact, edited by: Thierstein, H. R. and Young, J. R., Springer, Berlin, 99–125, 2004.

Rouco, M., Branson, O., Lebrato, M., and Iglesias-Rodríguez, M.: The effect of nitrate and phosphate availability on *Emiliania huxleyi* (NZEH) physiology under different CO_2 scenarios, Front. Microbiol., 4, 1–11, doi: 10.3389/fmicb.2013.00155, 2013.

Roy, R. N., Roy, L. N., Vogel, K. M., Porter-Moore, C., Pearson, T., Good, C. E., Millero, F. J., and Campbell, D. C.: Thermodynamics of the dissociation of boric acid in seawater at S 5 35 from 0 degrees C to 55 degrees C, Mar. Chem., 44, 243–248, doi: 10.1016/0304-4203(93)90206-4, 1993.

Shemi, A., Schatz, D., Fredricks, H. F., Van Mooy, B. A. S., Porat, Z., and Vardi, A.: Phosphorus starvation induces membrane remodeling and recycling in *Emiliania huxleyi*, New Phytol., 211, 886–898, doi: 10.1111/nph.13940, 2016.

https://doi.org/10.5194/egusphere-2022-947
Preprint. Discussion started: 10 October 2022

824 Solórzano, L., and Sharp, J. H.: Determination of total dissolved phosphorus and
825 particulate phosphorus in nature waters, Limnol. Oceanogr., 25, 754–758, doi:
826 10.4319/lo.1980.25.4.0754, 1980.
827 Steinacher, M., Joos, F., Frölicher, T. L., Bopp, L., Cadule, P., Cocco, V., Doney, S.
828 C., Gehlen, M., Lindsay, K., Moore, J. K., Schneider, B., and Segschneider, J.:
829 Projected 21st century decrease in marine productivity: a multi-model analysis,
830 Biogeosciences, 7, 979–1005, doi: 10.5194/bg-7-979-2010, 2010.
831 Sterner, R. W., and Elser, J. J.: Ecological Stoichiometry: The Biology of Elements
832 from Molecules to the Biosphere, Princeton University Press, Princeton, 2002.
833 Terrats, L., Claustre, H., Cornec, M., Mangin, A., and Neukermans, G.: Detection of
834 coccolithophore blooms with BioGeoChemical-Argo floats, Geophys. Res. Lett.,
835 47, e2020GL090559, doi: 10.1029/2020GL090559, 2020.
836 Townsend, D. W., Keller, M. D., Holligan, P. M., Ackleson, S. G., and Balch, W. M.:
837 Blooms of the coccolithophore *Emiliania huxleyi* with respect to hydrography in
838 the Gulf of Maine, Cont. Shelf Res., 14, 979–1000, doi:
839 10.1016/0278-4343(94)90060-4, 1994.
840 Tyrrell, T., and Merico, A.: *Emiliania huxleyi*: bloom observations and the conditions
841 that induce them, in: Coccolithophores : from molecular biology to global impact,
842 edited by: Thierstein, H. R. and Young, J. R., Springer, Berlin, 75–97, 2004.
843 Wang, C., Wang, J., Li, L., Wang, Y., and Lin, S.: P-limitation promotes carbon
844 accumulation and sinking of *Emiliania huxleyi* through transcriptomic
845 reprogramming, Front. Mar. Sci., 9, 860222, doi: 10.3389/fmars.2022.860222,
846 2022.
847 Wang, G., Xie, S. P., Huang, R. X., and Chen. C.: Robust warming pattern of global
848 subtropical oceans and its mechanism, J. Climate, 28, 8574–8584, doi:

https://doi.org/10.5194/egusphere-2022-947
Preprint. Discussion started: 10 October 2022

10.1175/jcli-d-14-00809.1, 2015.

Zhang, Y., Collins, S., and Gao, K.: Reduced growth with increased quotas of particulate organic and inorganic carbon in the coccolithophore *Emiliania huxleyi* under future ocean climate change conditions, Biogeosciences, 17, 6357–6375, doi: 10.5194/bg-17-6357-2020, 2020.

Zhang, Y., Li, Z. K., Schulz, K. G., Hu, Y., Irwin, A. J., and Finkel, Z. V.: Growth-dependent changes in elemental stoichiometry and macromolecular allocation in the coccolithophore *Emiliania huxleyi* under different environmental conditions, Limnol. Oceanogr., 66, 2999–3009, doi: 10.1002/lno.11854, 2021.

https://doi.org/10.5194/egusphere-2022-947
Preprint. Discussion started: 10 October 2022

Figure Legends

Figure 1. Growth rate (**a**, **b**), cellular contents of particulate organic carbon (POC, **c**, **d**), nitrogen (PON, **e**, **f**) and phosphorus (POP, **g**, **h**), and particulate inorganic carbon (PIC, **i**, **j**) of *Emiliania huxleyi* RCC1266 in the treatments of high phosphorus availability and low CO_2 level (HP+LC), high phosphorus availability and high CO_2 level (HP+HC), low phosphorus availability and low CO_2 level (LP+LC), and low phosphorus availability and high CO_2 level (LP+HC) under low light (left, 40 μmol photons m^{-2} s^{-1}) and high light (right, 300 μmol photons m^{-2} s^{-1}) intensities. Different letters represent significant differences in each parameters between treatments ($p < 0.05$). The data represents the means and standard deviation of four independent cultures.

Figure 2. Cellular contents of carbohydrate (**a**, **b**) and protein (**c**, **d**), and the percentages of POC allocated to carbohydrate (**e**, **f**) and protein (**g**, **h**), and the percentage of PON allocated to protein (**i**, **j**) of *E. huxleyi* RCC1266 in the treatments of high phosphorus availability and low CO_2 level (HP+LC), high phosphorus availability and high CO_2 level (HP+HC), low phosphorus availability and low CO_2 level (LP+LC), and low phosphorus availability and high CO_2 level (LP+HC) under low light (left) and high light (right) intensities. Different letters represent significant differences in each parameters between treatments ($p < 0.05$). The data represents the means and standard deviation of four independent cultures. Please see figure 1 for more detailed information.

Figure 3. Cellular POC : POP ratio (**a**), PON : POP ratio (**b**), and protein content (**c**) of *E. huxleyi* RCC1266 as a function of growth rate, and cellular POC content as a

https://doi.org/10.5194/egusphere-2022-947
Preprint. Discussion started: 10 October 2022

function of carbohydrate (**d**) in the treatments of high phosphorus availability and low CO_2 level (HP+LC, □), high phosphorus availability and high CO_2 level (HP+HC, ○), low phosphorus availability and low CO_2 level (LP+LC, △), and low phosphorus availability and high CO_2 level (LP+HC, ◇) under low light (LL, empty) and high light (HL, fill) intensities. Each point indicates an individual replicate under each treatment. Please see figure 1 for more detailed information.

https://doi.org/10.5194/egusphere-2022-947
Preprint. Discussion started: 10 October 2022

Table 1. Carbonate chemistry parameters and dissolved inorganic phosphorus (DIP) concentration at the end of the incubation. The values are means ± standard deviation (sd) of four replicates. Respectively, LL and HL represent 40 and 300 µmol photons m^{-2} s^{-1} of photosynthetically active radiation (PAR), and HP and LP represent 4 and 0.43 µmol L^{-1} PO_4^{3-} at the beginning of the incubations.

			pCO_2 (µatm)	pH (total scale)	TA (µmol L^{-1})	DIC (µmol L^{-1})	HCO_3^- (µmol L^{-1})	CO_3^{2-} (µmol L^{-1})	DIP (µmol L^{-1})
LL	HP	LC	403±4	8.06±0.01	2346±23	2074±21	1861±18	200±2	3.20±0.03
		HC	881±20	7.77±0.01	2351±33	2216±32	2074±30	114±2	3.12±0.08
	LP	LC	329±4	8.13±0.01	2332±24	2024±22	1787±19	225±3	<0.04
		HC	730±8	7.84±0.01	2349±24	2189±23	2033±22	132±2	<0.04
HL	HP	LC	357±9	8.09±0.01	2235±41	1959±35	1749±30	199±6	2.86±0.06
		HC	791±7	7.80±0.01	2296±20	2151±20	2007±18	118±1	2.70±0.06
	LP	LC	303±4	8.16±0.01	2354±13	2024±11	1773±9	241±3	<0.04
		HC	735±19	7.83±0.01	2319±69	2162±65	2011±60	128±5	<0.04

https://doi.org/10.5194/egusphere-2022-947
Preprint. Discussion started: 10 October 2022

Table 2. Growth rate (d^{-1}), cellular contents of POC, PON, POP, PIC, carbohydrate (CHO) and protein (Pro) (pg $cell^{-1}$), and the ratios of POC : PON, POC : POP, PON : POP and PIC : POC, and the percentages of POC allocated to carbohydrate (CHO–C : POC) and protein (Pro–C : POC), and the percentage of PON allocated to protein (Pro–N : PON) (%). LC and HC represent low CO_2 (426 μatm) and high CO_2 (946 μatm) levels, respectively. Please see table 1 for more detailed information.

	Low light intensity				High light intensity			
	HP		LP		HP		LP	
	LC	HC	LC	HC	LC	HC	LC	HC
Growth rate	0.91±0.03	0.88±0.01	0.83±0.02	0.70±0.03	1.35±0.03	1.33±0.02	1.34±0.02	1.12±0.02
POC	8.34±0.57	8.73±0.32	8.20±0.36	8.04±0.24	10.53±0.70	11.04±0.42	11.73±0.19	12.70±0.50
PON	1.49±0.16	1.58±0.12	1.23±0.06	1.20±0.10	1.65±0.05	1.89±0.07	1.51±0.07	1.56±0.06
POP	0.16±0.01	0.15±0.01	0.08±0.01	0.07±0.01	0.22±0.01	0.21±0.01	0.12±0.01	0.10±0.01
PIC	2.12±0.22	1.45±0.17	2.44±0.11	2.06±0.37	3.74±0.22	2.41±0.41	4.83±0.34	3.79±0.49
POC:PON	6.57±0.43	6.46±0.52	7.78±0.46	7.87±0.54	7.45±0.28	6.83±0.32	9.09±0.44	9.50±0.11
POC:POP	133.3±7.8	153.8±13.9	282.4±31.2	313.0±40.5	124.2±3.5	137.8±8.5	259.7±23.2	316.9±30.4
PON:POP	20.40±2.53	23.98±3.37	36.30±3.54	40.10±7.42	16.68±0.47	20.21±1.47	28.63±2.80	33.33±2.85
PIC:POC	0.26±0.04	0.17±0.02	0.30±0.02	0.26±0.04	0.36±0.02	0.22±0.04	0.41±0.03	0.30±0.04
CHO	1.45±0.15	1.81±0.16	1.79±0.16	1.94±0.16	3.58±0.41	4.30±0.17	4.96±0.24	5.85±0.49
Protein	5.23±0.55	5.37±0.39	3.73±0.27	3.80±0.15	6.45±0.36	6.97±0.22	6.25±0.29	6.28±0.30
CHO–C:POC	6.95±0.41	8.31±0.85	8.71±0.70	9.64±0.58	13.62±1.43	15.60±0.98	16.92±1.04	18.39±0.96
Pro–C:POC	33.26±3.24	32.58±1.98	24.15±2.52	25.07±1.69	32.49±1.69	33.51±1.41	28.23±1.35	26.21±1.27
Pro–N:PON	56.84±8.96	54.55±6.51	48.41±2.46	51.07±5.40	62.62±2.88	59.12±1.21	66.35±4.06	64.44±2.73

https://doi.org/10.5194/egusphere-2022-947
Preprint. Discussion started: 10 October 2022

961

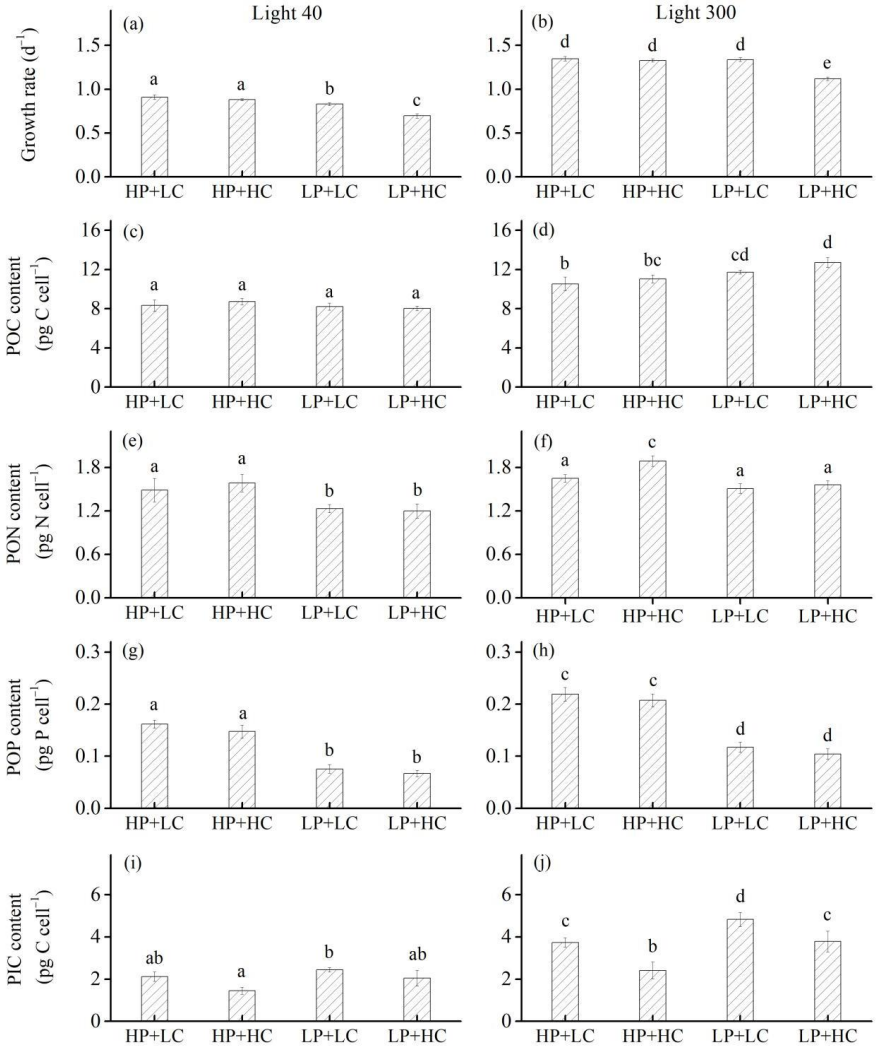

962

963

964 Figure 1

965

966

https://doi.org/10.5194/egusphere-2022-947
Preprint. Discussion started: 10 October 2022

967

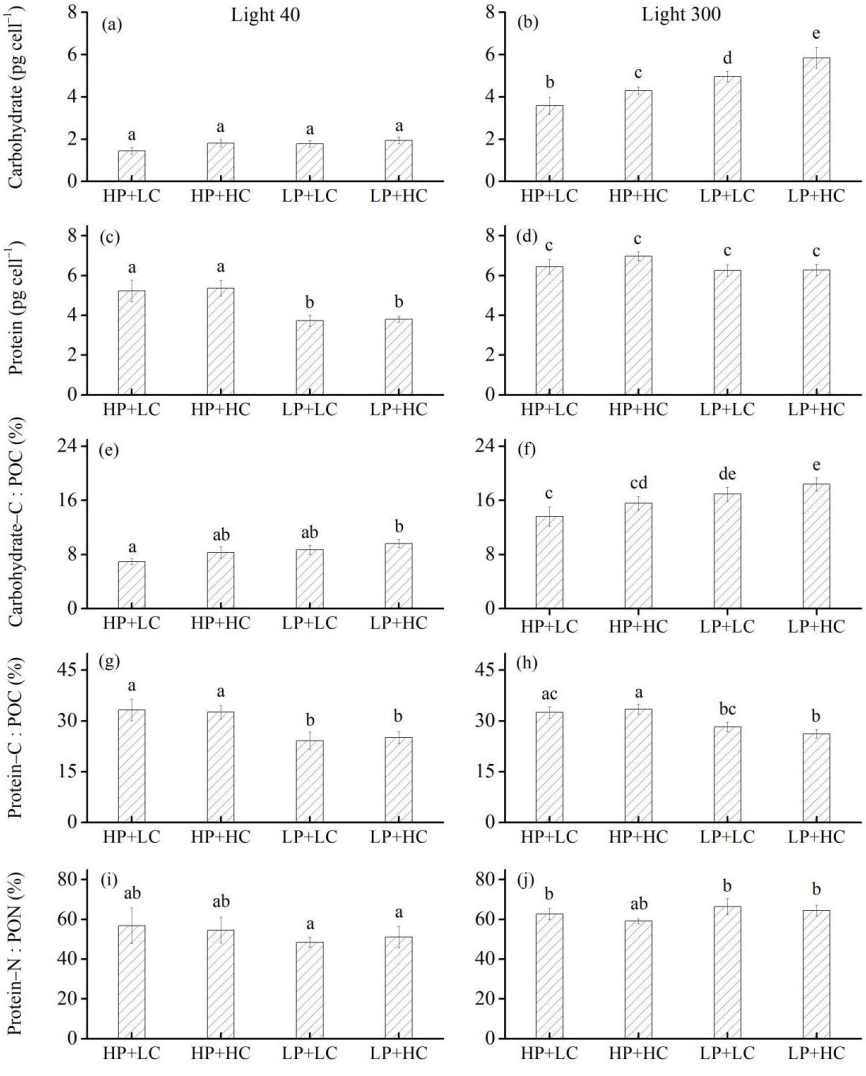

968

969

970 Figure 2

971

972

https://doi.org/10.5194/egusphere-2022-947
Preprint. Discussion started: 10 October 2022

973

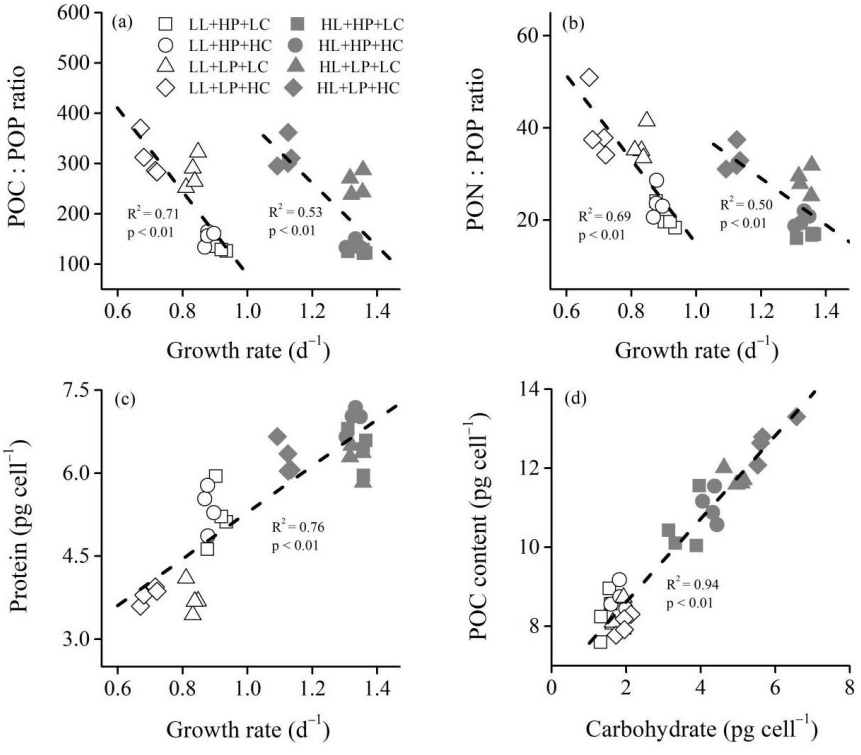

974

975

976 Figure 3

977

978